

論文97-34S-5-1

기지국 안테나 배열을 이용한 FDD 방식의 무선통신 시스템에서 송신 빔 형성을 위한 주파수 변환 방식

(Frequency Translation Approach for Transmission Beamforming in FDD Wireless Communication Systems with Basestation Arrays)

吳 成 根 * , Shawn P. Stapleton **

(Seong Keun Oh and Shawn P. Stapleton)

요 약

본 논문에서는 배열 안테나 송신 링크의 신호의 질(質)을 개선하기 위하여 적응 안테나 배열을 사용하는 주파수 분할 동시 송수신 방식(Frequency-division-duplex : FDD)의 무선통신 시스템을 위한 전송 빔 형성 기법들을 다룬다. 상향 링크 채널 벡터로부터 송신 빔 형성 가중치들을 도출해 내기 위하여 근사적인 주파수 변환법에 기초를 둔 간단하고 효과적인 송신 빔 형성 기법을 제안하였다. 이 기법은 단기 평균된 고속 페이딩 현상의 통계적인 특성들의 소폭 주파수 변환에 의한 불변성을 이용하였으며, 이를 위하여 송수신 채널 벡터들에 대한 간단한 근사 관계식이 유도되었다. 또한, 입사각 평균치 대신에 상향 링크 합성 각(角) 스펙트럼의 최대값에 해당하는 입사각을 이용하여 채널 벡터의 주파수 변환을 수행하는 보다 실질적인 기법을 제안하였다. 제안된 기법들의 성능을 분석하기 위하여 진(眞) 하향 링크 채널 벡터 대신에 채널 벡터 추정치를 이용함으로써 생기는 송신 링크 전력 손실이 평가 척도로 사용되었고, 입사각 평균치와 각 확산, 안테나 갯수, 송수신 주파수의 차이, 입사각 분포에 따른 성능 분석이 이루어졌다. 제안된 기법들의 성능은 기존의 직접 가중치 재사용 방법 및 입사각들을 이용한 송신 빔 형성법의 성능과 전력 손실면에서 비교되었다.

Abstract

We consider transmission beamforming techniques for frequency-division-duplex (FDD) wireless communication systems using adaptive arrays to improve the signal quality of the array transmission link. We develop a simple effective transmission beamforming technique based on an approximated frequency translation (AFT) to derive the transmission beamforming weights from the uplink channel vector. This technique exploits the invariance of the short-time averaged fast fading statistics to small frequency translations. A simple approximate relationship that relates the transmission channel vector to the reception channel vector is derived. We have developed its practical alternative in which the frequency translation of the channel vector is performed at the principal angle of arrival (AOA) of the uplink synthetic angular spectrum instead of the mean AOA. To analyze the performance of the proposed methods, we consider the power loss incurred by applying the estimated channel vector instead of the true downlink channel vector. The performance is analyzed as a function of the mean AOA, the angular spread, the number of elements, frequency difference between the uplink and the downlink, and the angle distribution. Their performance is also compared with that of the direct weight reuse method and the AOA based methods.

* 正會員, 亞洲大學校 電氣電子工學部
(School of Electrical and Electronic Engineering,
Ajou University)

** School of Eng. Science, Simon Fraser Univ.
接受日字: 1997年3月7日, 수정완료일: 1997年5月2日

I. Introduction

In mobile communication systems, the smart antenna system can increase the channel capacity and/or improve the signal quality by steering an optimum directional beam toward the direction of a desired user, while steering pattern nulls toward the directions of other co-channel users. Various techniques have been proposed to increase the capacity of mobile communication networks by performing spatially selective reception and transmission with adaptive antenna arrays^{[1]-[7]}. However, most research into adaptive arrays has focused on the uplink or reverse link (i.e., mobile-to-base link assuming antenna array at the base station)^{[8]-[9]}, for the downlink or forward link, less research effort has been made^[10].

The objective of adaptive beamforming for uplink is to maximize the SINR of the received desired signal at the base station antenna array. This goal can be achieved by using training symbol assisted channel estimation or blind channel estimation techniques^{[8]-[9], [17]}. For the downlink, the objective is both to maximize the received signal strength at the desired mobile and to minimize the interference to other co-channel users, thus maximizing the downlink SINR. Unlike the uplink channel, however, there is no way to monitor directly some measure of a signal quality received at the desired mobile if feedback techniques and/or probing techniques are not adopted. If the downlink channel vector was known, the downlink SINR could be maximized by multiplying the desired signal with a set of optimum downlink weights. Therefore, the problem in the downlink beamforming is how closely we can get an estimate of the downlink channel vector.

In time-division duplex(TDD) systems such as CT2/CT2+, DECT, and PHP, the downlink weights estimated during the reception can be re-used for the uplink weights, provided that the channel is relatively static during the time separation between reception and transmission^[3].

^[10]. In this case, the downlink weights are a scaled version of the uplink weights. However, in FDD systems such as IS-54, IS-95, and GSM, the concept of weight reuse can not be applied, since the frequency separation between the downlink and the uplink makes the downlink channel fading become uncorrelated with the uplink channel fading. Therefore, techniques which can calculate the downlink weights without relying on the weight reuse must be developed to improve the downlink performance of FDD systems using antenna arrays. In the FDD systems, since information on the downlink channel is not usually available to the base station, we are forced to use the uplink channel information to compute the downlink beamforming weights.

In recent years, several efforts have been attempted to estimate the downlink channel vector. One approach is the direct channel sounding technique in which the downlink channel vector is measured by using direct sounding and/or feedback techniques^{[10]-[11]}. But, these require a complete redesign of protocols and signaling and/or additional hardware at both the mobile terminal and the base station. Several AOA-based approaches have been proposed^{[12]-[14]}. Their premise is that although the channel vectors are different at uplink and downlink frequencies, the AOAs remain relatively unchanged. Based on the AOA information, the downlink weights are generated by maximizing the downlink SINR. But these techniques can not reproduce faithfully the angular information of the uplink channel, especially in case of the distributed AOAs within a certain angular range, and require computationally demanding AOA estimation processes. A similar approach is to use fixed or steerable multiple beams for both reception and transmission at the base station^[15], in which the strongest beam in uplink is selected and it will be used for downlink beamforming. But this approach is not optimal. In^[16], Raleigh et al. have proposed subspace mapping method that exploits the invariance channel properties between the uplink and downlink channels under two fundamental

observations: 1) Short-time averaged fast fading statistics are invariant to small frequency translations and 2) With properly chosen array geometry and a confined path angle spread, averaged array response vectors are also largely invariant to small frequency translations. Under the above observations, the scaled principal eigenvector of the receive covariance matrix is used as the transmit weight vector. However, this direct reuse of the scaled principal eigenvector of the uplink covariance matrix brings on still large power degradations.

In this paper, we develop an effective transmission beamforming method based on an approximated frequency translation to derive the transmission beamforming weights from the uplink channel vector. This technique exploits the invariance of the short-time averaged fast fading statistics to small frequency translations. A simple approximate relationship that relates the transmission channel vector to the reception channel vector is derived, in which the downlink beamforming weights are obtained by phase-rotating elements of the uplink channel vector at the mean AOA. But this techniques does not require knowledge on the specific AOAs. For its practical implementation, we develop a practical version in which the mean AOA estimate is replaced by the principal AOA corresponding to a peak of the uplink synthetic angular spectrum. To analyze the performance of the proposed methods, we consider the power loss incurred by applying the estimated channel vector instead of the true downlink channel vector. The performance is analyzed as a function of the mean AOA, the angular spread, the number of elements, frequency difference between the uplink and the downlink, and the angle distribution. Their performance also is compared with that of the direct weight reuse method and the AOA based methods.

This paper is organized as follows. Section II describes the vector channel models for uplink and downlink and describes the problem. A basic frequency translation algorithm for transmission beamforming and its practical alternative are

presented in Section III. Section IV shows the performance of these methods. Finally, we make conclusions in Section V.

II. Vector Channel Models and Problem Description

1. Uplink Vector Channel

Consider a vector channel model from the mobile transmitter with a single antenna to an antenna array at the base station. For simplicity, we consider only azimuth angles, but the results can be extended to consider the three-dimensional problem. An illustration of the vector channel is shown in Fig. 1. Radiation from the mobile illuminates all local scatterers, or local reflectors, surrounding the mobile within a few hundred wavelengths from the mobile. Reflected radiation from these local reflectors and/or the mobile reaches the base station either directly or by reflection from large reflecting objects (i.e., dominant reflectors) such as large buildings, hills, and mountains. Each reflected wave impinges on the antenna array at the base station with a certain AOA with respect to the base coordinate system.

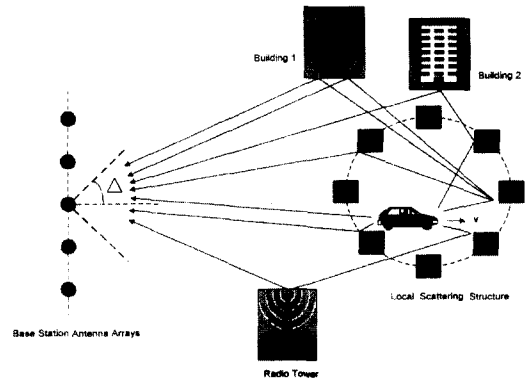


그림 1. 기지국 안테나 배열을 가진 전형적인 이동통신 환경에서의 벡터 채널의 예.

Fig. 1. Illustration of a typical mobile vector channel with basestation antenna array.

The received complex baseband signal vector at the base station antenna array is given by

$$\mathbf{x}(t) = \sum_{l=1}^L \mathbf{a}_r(\theta_l(t), \omega_r) \beta_l(t, \omega_r) s(t - \tau_l) + \mathbf{n}(t), \quad (1)$$

where $\mathbf{a}_r(\theta_l(t), \omega_r)$ denotes the base station array response vector corresponding to the AOA of the l -th path signal, $\theta_l(t)$ and the uplink frequency ω_r ; $\beta_l(t, \omega_r)$ denotes a Gaussian random process which represents fading behavior of the uplink channel; $s(t)$ is the transmitted complex baseband signal from the mobile; τ_l is the relative time delay corresponding to the l -th path; and $\mathbf{n}(t)$ is an additive Gaussian noise vector at the base station receiver.

The above model assumes that all the significant incoming signals arrive at the base station antenna array with L distinct angles of arrival. In this paper, instead of the distinct angle model, we consider a distributed angle model in which the received signals at the base station antenna are composed of a large number of indistinguishable paths within a given range of angles, $\pm \Delta$ of the mean AOA, θ_0 . The value of 2Δ is called as the angular spread around θ_0 . Assuming a narrowband signal, we can express as $s(t - \tau_l) \approx s(t - \tau_0)$, where $\tau_0 \in [\min_l \tau_l, \max_l \tau_l]$. Also, the short-time stationarity, that is, the channel is stationary for the time separation between signal reception and transmitting back, lets us be possible to delete the time dependency of the channel parameters such as fading components and AOAs of the incoming paths, from the vector channel model.

From the distributed angle model and the short-time stationarity, the distinct time-varying fading behaviors at the distinct angles are replaced by a distributed time-invariant angle distribution $p(\theta)$ within $\pm \Delta$ of the mean AOA θ_0 . Then, the baseband received signal vector in (1) can be rewritten as

$$\mathbf{x}(t) = s(t - \tau_r) \cdot \int_{\theta_0 - \Delta}^{\theta_0 + \Delta} p(\theta) \mathbf{a}_r(\theta, \omega_r) d\theta + \mathbf{n}(t). \quad (2)$$

From (2), we define the uplink channel vector $\mathbf{w}_r(\omega_r)$ as

$$\mathbf{w}_r(\omega_r) = \int_{\theta_0 - \Delta}^{\theta_0 + \Delta} p(\theta) \mathbf{a}_r(\theta, \omega_r) d\theta. \quad (3)$$

In what follows, for notational convenience, we delete the frequency dependency at the uplink channel vector and the array response vector, thus expressing $\mathbf{x}_r(\omega_r)$ and $\mathbf{a}_r(\theta, \omega_r)$ as \mathbf{w}_r and $\mathbf{a}_r(\theta)$, respectively.

2. Downlink Vector Channel

Downlink vector channel can be modeled in a similar way as in the above uplink channel with the exception of the transmission from the base station antenna array with M elements to the single mobile antenna. We again assume the short-time stationarity, the distributed angle model and the narrowband signal. Instead of the invariance of the short-time averaged array response vectors or covariance matrices^[16], we assume the AOA reciprocity^{[12]-[14]} between the uplink and the downlink with a small frequency translation. From this, for a time interval between signal reception and transmitting back, we assume that the uplink and the downlink have an identical angle distribution. Under these assumptions, only difference between the uplink and the downlink is the carrier frequency. Hence, the downlink channel vector $\mathbf{x}_t(\omega_t)$ is defined as

$$\mathbf{x}_t(\omega_t) = \int_{\theta_0 - \Delta}^{\theta_0 + \Delta} p(\theta) \mathbf{a}_t(\theta, \omega_t) d\theta. \quad (4)$$

where $\mathbf{a}_t(\theta, \omega_t)$ is the downlink array response vector of the base station array corresponding to the radiating angle θ at the downlink frequency ω_t ; and $n_m(t)$ denotes an additive Gaussian noise at the mobile receiver. In what follows, for notational convenience, we express again $\mathbf{w}_t(\omega_t)$ and $\mathbf{a}_t(\theta, \omega_t)$ as \mathbf{w}_t and $\mathbf{a}_t(\theta)$, respectively.

3. Downlink Beamforming

In the FDD downlink adaptive array problem, the objective is to determine the optimum transmission beamforming weights which maximize the radiation toward the desired mobile while minimizing the radiation toward other co-channel mobiles. To perform the optimum downlink beamforming, all the downlink channel

vectors from the base to all the mobiles must be known. In practice, it is not possible to measure an individual downlink channel vector without any additional hardware, protocol change, interruption of the operation and/or performance loss. From the AOA reciprocity, an individual channel vector can be estimated from its corresponding uplink channel vector which can be obtained by using training symbol assisted channel estimation or blind channel estimation techniques^{[8]-[10],[17]}.

If all the downlink channel vectors are known, we can determine the optimum downlink beamforming weights. Then the data signal is weighted with the optimum weights so that the received signal at the mobile is expressed as

$$y(t) = s(t - \tau) \cdot \mathbf{w}_{\text{opt}}^* \cdot \mathbf{w}_t + n_m(t), \quad (5)$$

where \mathbf{w}_{opt} is the optimum downlink beamforming weight vector. In a single user case, the optimum weight \mathbf{w}_{opt} is given simply by

$$\mathbf{w}_{\text{opt}} = \mathbf{w}_t. \quad (6)$$

In this paper, since we are interested in only how to determine the downlink channel vector from the uplink channel vector, the remaining part of this paper is devoted to one-to-one mapping problem between the uplink channel vector and the downlink channel vector.

III. Frequency Translation Algorithms

1. Mean AOA-Based Approximated Frequency Translation (AFT) Method

We develop an approximated frequency translation method that can provide a simple and accurate estimate of the downlink channel vector from the corresponding uplink channel vector by exploiting the AOA reciprocity between the uplink and downlink channels. Consider an array of M isotropic elements with arbitrary geometry. We begin by defining the downlink array response vector corresponding to the radiation angle θ , $\mathbf{a}_t(\theta)$ as

$$\mathbf{a}_t(\theta) = \left[1, e^{j2\pi \frac{d_{1,2}}{\lambda_t} \sin(\theta + \phi(2))}, \dots, e^{j2\pi \frac{d_{1,M}}{\lambda_t} \sin(\theta + \phi(M))} \right]^T. \quad (7)$$

where $d_{l,m}$ is the distance between element 1 and element m ; $\phi(m)$ denotes the anti-clockwise rotational angle between the reference axis crossing element 1 and the line joining element 1 and element m ; and λ_t is the wavelength of the transmit carrier.

From (4) and (7), we would examine the m -th element of the downlink channel vector

$$\mathbf{w}_t(m) = \int_{\theta_0 - \Delta}^{\theta_0 + \Delta} p(\theta) \mathbf{a}_t(\theta, m) d\theta. \quad (8.a)$$

$$= \int_{\theta_0 - \Delta}^{\theta_0 + \Delta} p(\theta) e^{j2\pi f_t \frac{d_{l,m}}{c} \sin(\theta + \phi(m))} d\theta, \quad (8.b)$$

$$= \int_{\theta_0 - \Delta}^{\theta_0 + \Delta} p(\theta) e^{j2\pi f_t \frac{d_{l,m}}{c} \sin(\theta + \phi(m))} e^{j2\pi(f_t - f_r) \frac{d_{l,m}}{c} \sin(\theta - \phi(m))} d\theta, \quad (8.c)$$

where c denotes the speed of light. Since $(f_t - f_r) / f_r \ll 1$ with small frequency translations, the effect of the angular spread in the second exponent of (8.c) is reduced by $(f_t - f_r) / f_r$ as compared to that of the first exponent. In a typical system with $f_r = 824$ to 849 MHz and $f_t - f_r = 45$ MHz, the factor becomes about $1/20$. Neglecting the effect of the angular spread due to the second exponent of (8.c), we can make the approximation

$$(f_t - f_r) \frac{d_{l,m}}{c} \sin(\theta + \phi(m)) \approx (f_t - f_r) \frac{d_{l,m}}{c} \sin(\theta_0 + \phi(m)), \quad \theta_0 - \Delta \leq \theta \leq \theta_0 + \Delta \quad (9)$$

Using (9), $w_t(m)$ can be approximated to

$$\begin{aligned} w_t(m) &\approx e^{j2\pi(f_t - f_r) \frac{d_{l,m}}{c} \sin(\theta_0 + \phi(m))} \\ &\cdot \int_{\theta_0 - \Delta}^{\theta_0 + \Delta} p(\theta) e^{j2\pi f_t \frac{d_{l,m}}{c} \sin(\theta + \phi(m))} d\theta, \quad (10) \\ &= e^{j2\pi(f_t - f_r) \frac{d_{l,m}}{c} \sin(\theta_0 + \phi(m))} \cdot w_r(m). \end{aligned}$$

Therefore, the downlink channel vector can be approximated as

$$\widehat{\mathbf{w}}_t = \Phi(\omega_t - \omega_r, \theta_0) \cdot \mathbf{w}_r, \quad (11)$$

where the rotational operator $\Phi(\omega_t - \omega_r, \theta_0)$ is a function of θ_0 and the frequency difference between the two channels, and is defined as

$$\Phi(\omega_t - \omega_r, \theta_0) = \text{diag} \left(1, e^{j2\pi(f_t - f_r) \frac{d_{1,2}}{c} \sin(\theta_0 + \phi(2))}, \dots, e^{j2\pi(f_t - f_r) \frac{d_{1,M}}{c} \sin(\theta_0 + \phi(M))} \right) \quad (12)$$

2. Principal AOA-Based AFT Method

Now, we consider the practical implementation issue. The proposed frequency translation method given in (11) and (12) requires the information about the mean AOA, θ_0 to construct the rotational operator matrix. In practice, it is not so easy to estimate the mean AOA. Hence, instead of the mean AOA, we consider the use of the principal AOA which represents the angle corresponding to the peak of the synthetic angular power spectrum of the uplink channel. The term “synthetic” is used because the angular spectrum must be computed from the uplink channel vector, and it is different from $p(\theta)$.

Consider the discrete synthetic angular spectrum of the uplink channel defined as

$$X_r(k) = \sum_{m=1}^M w_r(m) e^{-j\pi \frac{d_r m}{\lambda_r} \sin(\pi \frac{k}{K} + \phi(m))},$$

$k = -K, \dots, K$, integer. (13)

Then, the principal AOA index is obtained as

$$\hat{k}_{peak} = \max_{k \in \{-K, \dots, K\}} \{ \|X(k)\|^2 \}$$
 (14)

and its principal AOA estimate is computed as

$$\hat{\theta}_0 = \pi \cdot \hat{k}_{peak} / K. \quad (15)$$

For this method, the required spectral resolution K is not too large. From the results, $K=M$ is enough to give satisfactory performance.

The proposed AFT methods have a disadvantage that it can not make any rotation of the uplink channel vector near $\hat{\theta}_0 = -\phi(m)$, $m=1, \dots, M$. The effect is more serious in the uniform linear array in which all $\phi(m)=0$, $m=1, \dots, M$, thus resulting in no rotation in all the elements. It degrades the performance of these methods near $\hat{\theta}_0=0$ in the case where the true uplink channel vector disagrees with the downlink channel vector near $\hat{\theta}_0=0$ to a great extent.

IV. Results

To demonstrate the accuracy of the estimated

downlink channel vector obtained by the proposed methods, we consider the power loss at the mobile incurred by applying the estimated channel vector instead of the true one in the case of a single user FDD system. The power loss (L) is defined as

$$L = -20 \log_{10} \left\{ \frac{\|\mathbf{w}_t^H \cdot \hat{\mathbf{w}}_t\|}{\|\mathbf{w}_t\| \cdot \|\hat{\mathbf{w}}_t\|} \right\}, \quad (\text{dB}). \quad (16)$$

We consider a uniform linear array (ULA). We examine the effects on the mean AOA, the angular spread, the number of array elements, the frequency difference between the downlink and the uplink, and the angle distribution. The sensitivity to estimation error of the mean AOA is also investigated. The operating frequency ranges within 824 to 849 MHz for uplink (mobile-to-base station) and 869 to 894 MHz for downlink (base to mobile) with 45 MHz separation between the uplink channels and the corresponding downlink channels are considered.

In all the examinations except the effect on the frequency difference, we use the operating frequencies such as $f_{\max} = 894$ MHz, $f_t = 894$ MHz and $f_r = 849$ MHz. Also, we assume half-wavelength antenna spacing at the highest operating frequency. We compare the performance of the proposed methods with that of the direct weight reuse method and the AOA based method.

We first examine the effect on the mean AOA and the angular spread. For this, we consider the uniform angle distribution over $-\Delta$ to Δ around the mean AOA as follow:

$$p(\theta) = \begin{cases} \frac{1}{2\Delta}, & \theta_0 - \Delta \leq \theta \leq \theta_0 + \Delta. \\ 0, & \text{elsewhere} \end{cases} \quad (17)$$

We consider the angular spread range over $2\Delta = 0^\circ$ to 60° , typical for systems where the antenna array is located at the base station (including rural and urban areas) and $M=10$. Figs. 2, 3, 4 and 5 show the power loss profiles as a function of the mean AOA and the angular spread for the four different methods, the mean AOA-based AFT method, its peak AOA-based alternative, direct weight reuse method, and AOA-based method, respectively.

From these figures, we see that the performance of all the considered methods is severely dependent on both the mean AOA and the angular spread. We also see that the two proposed methods perform significantly better than the other two methods do. From Figs. 2 and 3, we see that the peak AOA-based AFT method performs as well as its mean AOA version does. We also see that the proposed methods work better as θ_0 approaches to $\pm 90^\circ$ and the angular spread decreases. These tendencies are obvious since $\sin \theta$ is less sensitive to variation of θ near $\theta = \pm 90^\circ$ and also the approximation in (9) is based on a smaller angular spread. But, the performance degradation of the two proposed methods within 60° uniform angular spread range is still negligible in most applications. In contrast, the performance for the direct weight reuse method becomes worse as θ_0 approaches to $\pm 90^\circ$ since there exists the largest phase difference between the downlink array response vector and the uplink one at $\theta = \pm 90^\circ$. From Figs. 2 and 4, it must be noted that the performance of the two methods at $\theta_0 = 0^\circ$ is identical as mentioned earlier. Finally, Fig. 5 shows that the performance of the single AOA-based method using the mean AOA is significantly degraded as the angular spread becomes larger, especially near $\theta_0 = 0^\circ$.

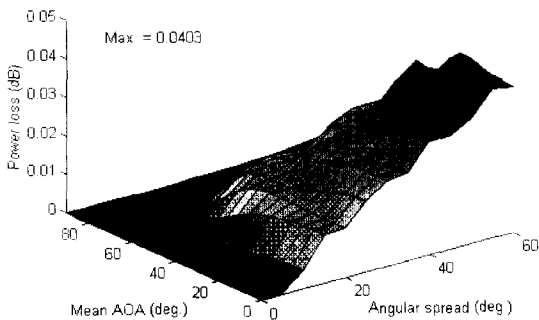


그림 2. 제안된 입사각 평균치를 이용한 AFT방법의 입사각 평균치와 각 확산에 따른 전력 손실 특성. $M=10$ 과 $f_t - f_r = 45$ MHz의 변수 값들이 사용됨.
 Fig. 2. Power loss profile as a function of the mean AOA and the angular spread for the proposed mean AOA-based AFT method, with $M=10$ and $f_t - f_r = 45$ MHz.

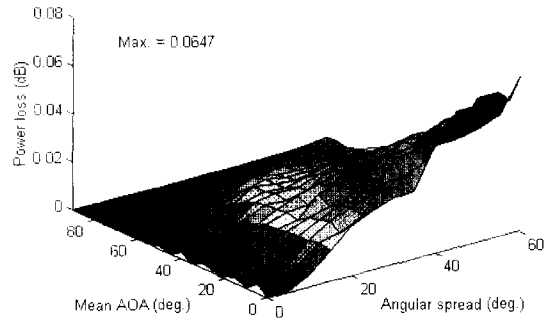


그림 3. 제안된 최대전력 입사각을 이용한 AFT방법의 입사각 평균치와 각 확산에 따른 전력 손실 특성. 변수 값들은 그림2와 같음.
 Fig. 3. Power loss profile as a function of the mean AOA and the angular spread for the proposed peak AOA-based AFT method, in the same environments as in Fig. 2.

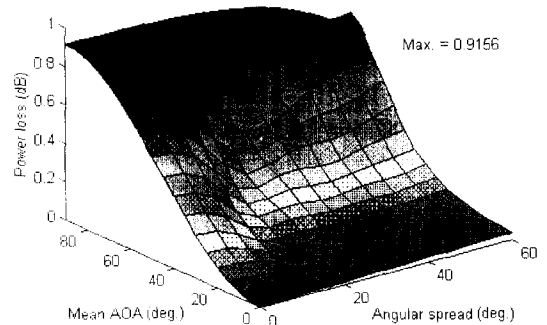


그림 4. 직접 가중치 재사용 방법의 입사각 평균치와 각 확산에 따른 전력손실 특성. 변수 값들은 그림 2와 같음.
 Fig. 4. Power loss profile as a function of the mean AOA and the angular spread for the direct weight reuse method, in the same environments as in Fig. 2.

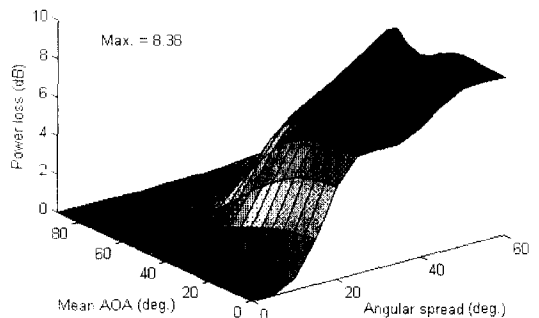


그림 5. 단일 입사각 방법의 입사각 평균치와 각 확산에 따른 전력 손실 특성. 변수 값들은 그림 2와 같음.
 Fig. 5. Power loss profile as a function of the mean AOA and the angular spread for the single AOA method, in the same environments as in Fig. 2.

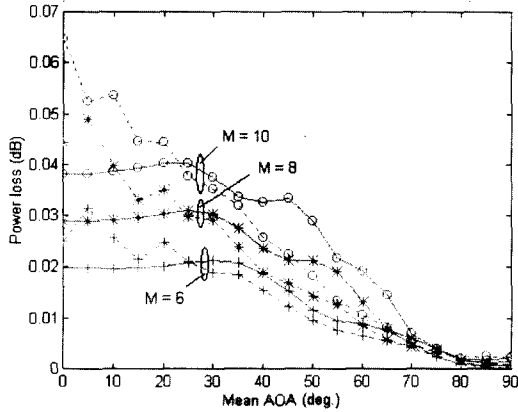


그림 6. 두가지 제안된 방법들의 M을 파라미터로 한 입사각 평균치에 따른 전력 손실. $2\Delta=60^\circ$ 과 $\theta_0=0^\circ$, $f_t - f_r = 45$ MHz의 변수 값들이 사용됨. (실선: 입사각 평균치 방법; 점선: 최대전력 입사각 방법)

Fig. 6. Power loss vs. the mean AOA with M as a parameter for the proposed two methods. The values of $2\Delta=60^\circ$, $\theta_0=0^\circ$, and $f_t - f_r = 45$ MHz are used. (Solid : Mean AOA-based method; Dotted : Peak AOA-based method)

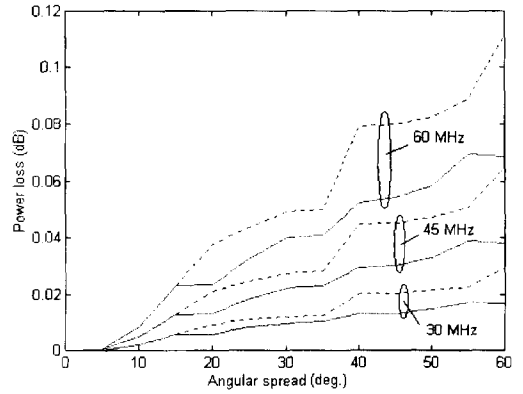


그림 8. 두가지 제안된 방법의 송수신 주파수 차이($f_t - f_r$)를 파라미터로 한 각 확산에 따른 전력 손실. $M=10$ 과 $\theta_0=0^\circ$ 의 변수 값들이 사용됨. (실선: 입사각 평균치 방법; 점선: 최대전력 입사각 방법)

Fig. 8. Power loss vs. the angular spread with the frequency difference $f_t - f_r$ as a parameter for the proposed two methods. The values of $M=10$ and $\theta_0=0^\circ$ are used. (Solid : Mean AOA-based method; Dotted : Peak AOA-based method)

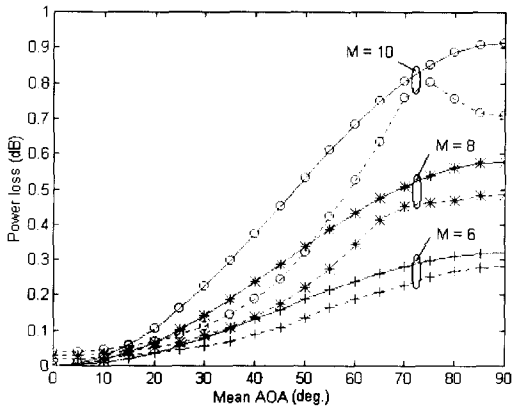


그림 7. 직접 가중치 재사용 방법의 M과 각 확산 값들을 파라미터로 한 입사각 평균치에 따른 전력 손실. $\theta_0=90^\circ$, $f_t - f_r = 45$ MHz의 변수 값들이 사용됨. (실선: $2\Delta=0^\circ$; 점선: $2\Delta=60^\circ$)

Fig. 7. Power loss vs. the mean AOA with M and the angular spread as parameters for the direct weight reuse method. The values of $\theta_0=90^\circ$ and $f_t - f_r = 45$ MHz are used. (Solid : $2\Delta=0^\circ$; Dotted : $2\Delta=60^\circ$)

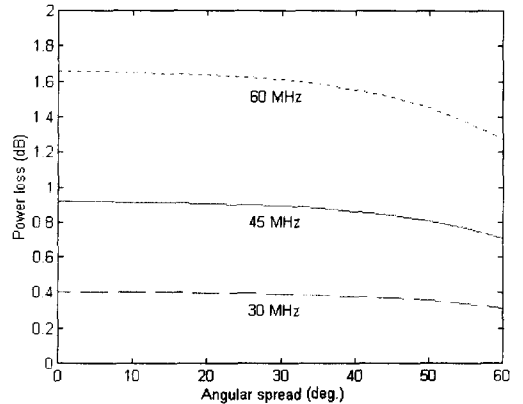


그림 9. 직접 가중치 재사용 방법의 송수신 주파수 차이를 파라미터로 한 각 확산에 따른 전력 손실. $M=10$ 과 $\theta_0=90^\circ$ 의 변수 값들이 사용됨.

Fig. 9. Power loss vs. the angular spread with the frequency difference $f_t - f_r$ as a parameter for the direct weight reuse method. The values of $M=10$ and $\theta_0=90^\circ$ are used.

To see the effect of the number of elements, we consider two different angular spread values, $2\Delta = 0^\circ$ and $2\Delta = 60^\circ$, and the uniform angle distribution as in (17). Figs. 6 and 7 show the power loss performance of the proposed methods and the direct weight reuse method, respectively, as a function of θ_0 with M and Δ as parameters. In all the considered methods, as expected, the performance becomes degraded as M increases. From Fig. 6, the proposed methods show excellent performance over various values of M .

The effect of the frequency difference on the power loss performance is shown in Figs. 8 and 9 for the proposed methods and the direct weight reuse method, respectively. For this, we consider again the uniform angle distribution and $M=10$. From these figures, we see the expected result that the performance is severely degraded as the frequency difference becomes larger. But, as shown in Fig. 8, the power loss of the two proposed methods is still less than 0.1 dB, even with 60 MHz frequency difference.

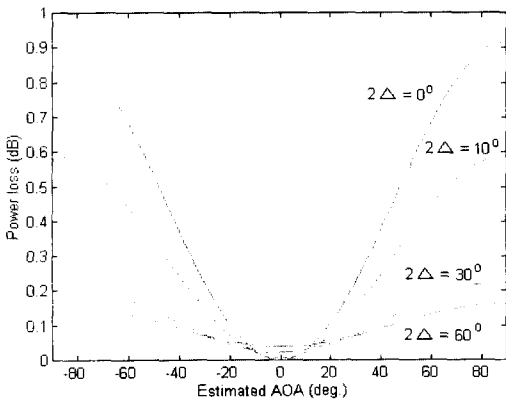


그림 10. 입사각 평균치 AFT 방법의 각 확산을 파라미터로 한 입사각 평균치 오차에 따른 감도. $M=10$ 과 $\theta_0=90^\circ$, $f_t - f_r = 45$ MHz의 변수 값들이 사용됨.

Fig. 10. Sensitivity to the mean AOA error with the angular spread as a parameter for the mean AOA-based AFT method. The values of $M=10$, $\theta_0=90^\circ$ and $f_t - f_r = 45$ MHz are used.

Fig. 10 shows the sensitivity of the mean AOA-based AFT method to the mean AOA

estimation error at $\theta_0=0^\circ$. The sensitivity does not determine only the degree of performance degradation as a function of angular spread in the distinct angle model with only a few paths, but also the degree of performance degradation of the peak AOA-based method.

Finally, we consider the distinct angle model to examine the effect of the proposed methods on the angle distribution as follows. The distinct angle model consists of a sum of three equally spaced distinct paths with different magnitude, in which each path has a uniform angle distribution within $\pm\Delta$ of its center angle, and is defined as

$$p(\theta) = c \cdot \begin{cases} \frac{\alpha_1}{2\Delta}, & \theta_0 - \Delta \leq \theta \leq \theta_0 + \Delta, \\ \frac{\alpha_2}{2\Delta}, & \theta_0 + \theta_s - \Delta \leq \theta \leq \theta_0 + \theta_s + \Delta, \\ \frac{\alpha_3}{2\Delta}, & \theta_0 - \theta_s - \Delta \leq \theta \leq \theta_0 - \theta_s + \Delta, \\ 0, & \text{elsewhere,} \end{cases} \quad (18)$$

where θ_0 is the mean AOA and also is the center angle of central path; θ_s denotes an angle separation from θ_0 in both directions; c is a normalization constant; α_1 , α_2 , and α_3 are the path amplitudes of the central path, the right path, and the left path, respectively. In this analysis, we use three different amplitudes as $\alpha_1=1.0$, $\alpha_2=0.866$ and $\alpha_3=0.5$, and consider two different angle spread values, $2\Delta=5^\circ$ and 10° . The remaining parameters used are given as follows: $M=10$, $f_t - f_r = 45$ MHz. We have analyzed the performance of five different methods as follows: The mean AOA-based AFT method, its peak AOA-based alternative, the direct weight reuse method, the matched amplitude AOA-based method, and the equal amplitude AOA-based method. The last two methods assume the exact knowledge on the center AOAs of each path, and for the matched amplitude AOA-based method, the exact amplitudes of individual paths is used to synthesize the transmission beamforming weights, while the equal amplitude method uses the equal amplitudes for all the three paths.

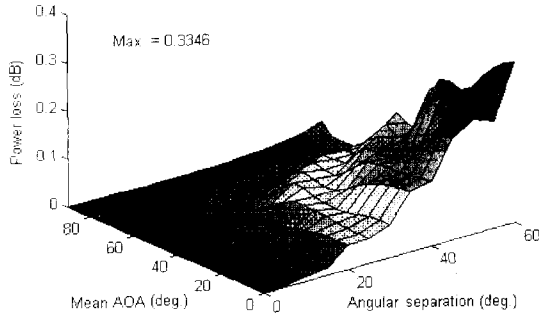


그림 11. 입사각 평균치를 이용한 AFT방법의 분리된 경로 신호들에 대한 입사각 평균치와 각 확산에 따른 전력 손실 특성. $M=10$ 과, $2\Delta=5^\circ$, $f_t - f_r = 45$ MHz의 변수 값들이 사용됨.

Fig. 11. Power loss profile as a function of the mean AOA and the angle separation of the distinct path signals for the mean AOA-based AFT method. The values of $M=10$, $2\Delta=5^\circ$, and $f_t - f_r = 45$ MHz are used.

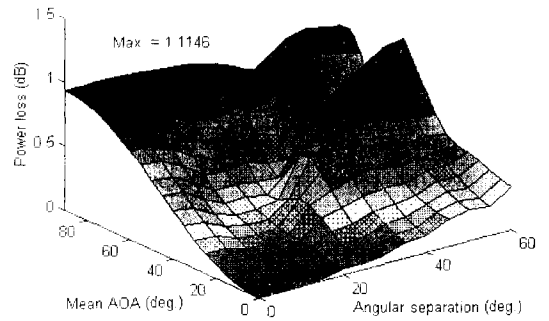


그림 13. 직접 가중치 재사용 방법의 분리된 경로 신호들에 대한 입사각 평균치와 각 확산에 따른 전력 손실 특성. 변수 값들은 그림11에서와 같음.

Fig. 13. Power loss profile as a function of the mean AOA and the angle separation of the distinct path signals for the direct weight reuse method, in the same environments as in Fig. 11.

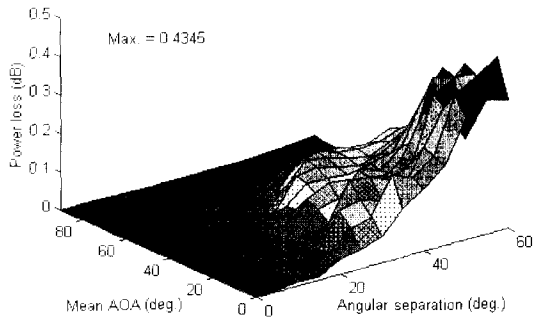


그림 12. 최대전력 입사각을 이용한 AFT방법의 분리된 경로 신호들에 대한 입사각 평균치와 각 확산에 따른 전력 손실 특성. 변수 값들은 그림11에서와 같음.

Fig. 12. Power loss profile as a function of the mean AOA and the angle separation of the distinct path signals for the peak AOA-based AFT method, in the same environments as in Fig. 11.

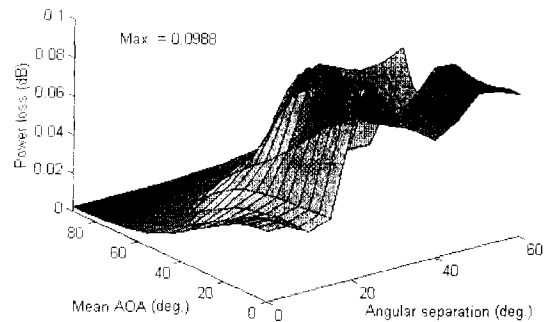


그림 14. 진폭 정합된 방법의 분리된 경로 신호들에 대한 입사각 평균치와 각 확산에 따른 전력 손실 특성. 변수 값들은 그림11에서와 같음.

Fig. 14. Power loss profile as a function of the mean AOA and the angle separation of the distinct path signals for the matched amplitude AOA-based method, in the same environments as in Fig. 11.

Figs. 11 through 15 and Figs. 16 through 20 show the power loss profiles of the above five different methods as a function of θ_0 and the total angle separation $2\theta_s$, with $2\Delta=5^\circ$ and 10° , respectively. From Figs. 11 through 13, the power losses of the proposed methods over all the considered cases is less than 0.5 dB even with $\theta_s = 30^\circ$, while the loss of the direct weight reuse

method is getting close to 1.5 dB. The 0.5 dB loss for the proposed methods with $M=10$ may still be acceptable in most applications. For the AOA-based methods, as expected, the matched amplitude method performs better than the equal magnitude method in small angle spread case. From Figs. 11, 12, 14, and 15, the AOA-based methods performs better than the two proposed

methods do. But, the proposed AFT methods seem slightly better than the equal amplitude AOA-based method. The performance of the AOA-based methods would be degraded further if the AOA estimates and the amplitude estimates instead of the true values are used.

In the case of $2\Delta=10^\circ$, the power losses of the proposed methods are reduced to below 0.3 dB. In

contrast, the power losses of the AOA-based methods are close to 1.0 dB, irrespective of amplitude matching, thereby producing severe degradation as the angle spread becomes larger. But, the performance of the direct weight reuse method is not sensitive to the angle spread variation.

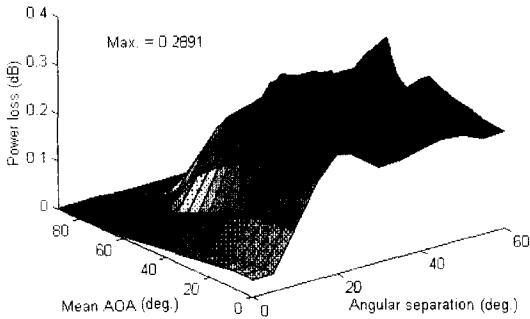


그림 15. 동일 진폭 입사각 방법의 분리된 경로 신호들에 대한 입사각 평균치와 각 확산에 따른 전력 손실 특성. 변수 값들은 그림11에서와 같음.

Fig. 15. Power loss profile as a function of the mean AOA and the angle separation of the distinct path signals for the equal amplitude AOA-based method, in the same environments as in Fig. 11.

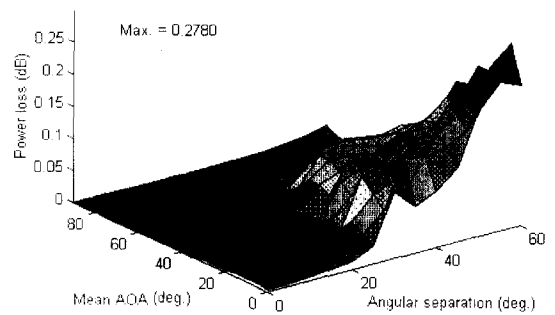


그림 17. 최대전력 입사각을 이용한 AFT방법의 분리된 경로 신호들에 대한 입사각 평균치와 각 확산에 따른 전력 손실 특성. 변수 값들은 그림16에서와 같음.

Fig. 17. Power loss profile as a function of the mean AOA and the angle separation of the distinct path signals for the peak AOA-based AFT method, in the same environments as in Fig. 16.

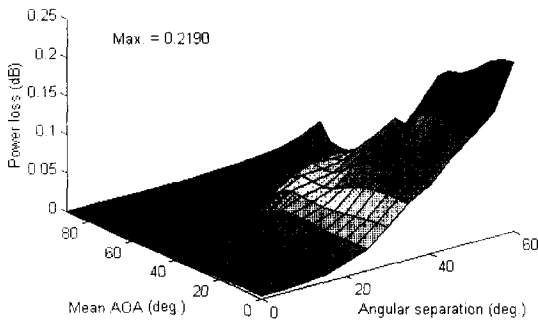


그림 16. 입사각 평균치를 이용한 AFT방법의 분리된 경로 신호들에 대한 입사각 평균치와 각 확산에 따른 전력 손실 특성. $2\Delta=10^\circ$ 가 사용됨. 나머지 변수 값들은 그림11에서와 같음.

Fig. 16. Power loss profile as a function of the mean AOA and the angle separation of the distinct path signals for the mean AOA-based AFT method, in the same environments as in Fig. 11 except for $2\Delta=10^\circ$.

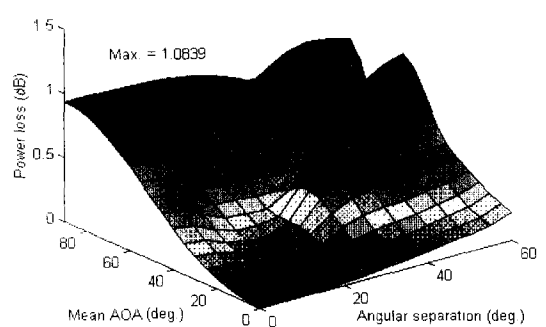


그림 18. 직접 가중치 재사용 방법의 분리된 경로 신호들에 대한 입사각 평균치와 각 확산에 따른 전력 손실 특성. 변수 값들은 그림16에서와 같음.

Fig. 18. Power loss profile as a function of the mean AOA and the angle separation of the distinct path signals for the direct weight reuse method, in the same environments as in Fig. 16.

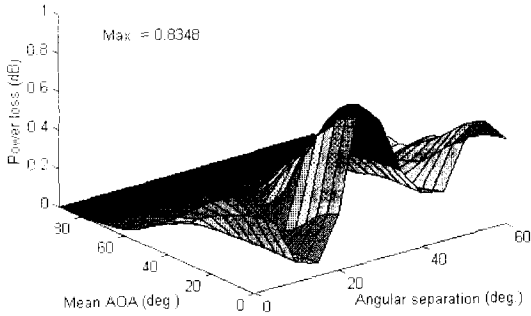


그림 19. 진폭 정합된 입사각 방법의 분리된 경로 신호들에 대한 입사각 평균치와 각 확산에 따른 전력 손실 특성. 변수 값들은 그림16에서와 같음.

Fig. 19. Power loss profile as a function of the mean AOA and the angle separation of the distinct path signals for the matched amplitude AOA-based method, in the same environments as in Fig. 16.

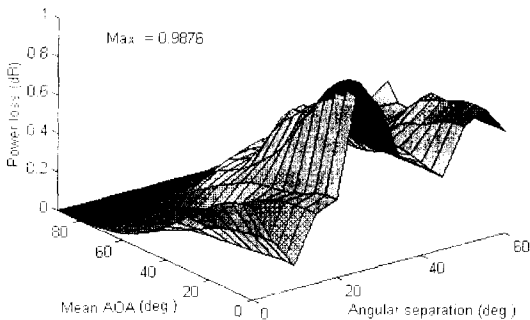


그림 20. 동일 진폭 입사각 방법의 분리된 경로 신호들에 대한 입사각 평균치와 각 확산에 따른 전력 손실 특성. 변수 값들은 그림16에서와 같음.

Fig. 20. Power loss profile as a function of the mean AOA and the angle separation of the distinct path signals for the equal amplitude AOA-based method, in the same environments as in Fig. 16.

From the results, we can conclude that the proposed methods are the most effective methods for the distributed AOA propagation channels. For the distinct AOA propagation channels with a few paths in which each path has a small angle spread and is separated from the other paths, the proposed methods give still satisfactory results. Their performance becomes improved as the number of paths increase and/or the angle spread of each

path becomes larger. Therefore, the proposed methods can be used as general approach in mobile communication systems with basestation antenna array for small frequency translations.

V. Conclusions

We have dealt with transmission beamforming problem for FDD wireless communication systems using adaptive arrays to improve the signal quality of the array transmission link. We developed the simple effective transmission beamforming method based on the approximated frequency translation to derive the transmission beamforming weights from the uplink channel vector. We derived the simple approximate relationship that relates the transmission channel vector to the reception channel vector. For implementation purpose, we developed the practical alternative in which the frequency translation of the channel vector is performed at the peak AOA of the uplink synthetic angular spectrum instead of the mean AOA. These techniques do not require the information on specific AOAs. As a proper performance measure, we considered the power loss incurred by applying the estimated channel vector instead of the true downlink channel vector.

The performance has been examined as a function of the mean AOA, the angular spread, the number of elements, frequency difference between the uplink and the downlink, and the angle distribution. Their performance also has been compared with that of the direct weight reuse method and the AOA-based methods. From the results, we conclude that the proposed methods are the most effective methods for the distributed AOA propagation channels. For the distinct AOA propagation channels with a few paths in which each path has a small angle spread and is largely separated from the other paths, the proposed methods give still satisfactory results. Their performance becomes improved as the number of paths increase and/or the angle spread of each path becomes larger. Therefore the proposed

methods can be used as general approaches in mobile communication systems with base station antenna arrays for small frequency translations.

Future investigations will include the analysis of the power loss performance in the case of the uniform circular array and the effect on the array calibration error, and the application to time-varying propagation channels to analyze the BER performance and the SNR degradation performance.

References

- [1] J. H. Winters, Optimum combining in digital mobile radio with cochannel interference, *IEEE J. Select. Areas in Comm.*, vol. SAC-2, no. 4, pp. 528-539, July 1984.
- [2] S. C. Swales, M. A. Beach, D. J. Edwards, and J. P. McGeehan, The performance enhancement of multibeam adaptive base station antennas for cellular land mobile radio systems, *IEEE Trans. Veh. Tech.*, vol. 39, no. 1, pp. 56-67, Feb. 1990.
- [3] S. Anderson, M. Millnert, M. Viberg, and Wahlberg, An adaptive array for mobile communication systems, *IEEE Trans. Veh. Tech.*, vol. 40, no. 1, pp. 230-236, Feb. 1991.
- [4] P. Balaban and J. Salz, Optimum diversity combining and equalization in data transmission with application to cellular mobile radio - Part I: Theoretical considerations, *IEEE Trans. Comm.*, vol. 40, no. 5, pp. 885-894, May 1992.
- [5] J. H. Winters, Signal acquisition and tracking with adaptive arrays in the digital mobile radio system IS-54 with flat fading, *IEEE Trans. Veh. Tech.*, vol. 42, no. 4, pp. 377-384, Nov. 1993.
- [6] A. F. Naguib, A. Paulraj, and T. Kailath, Capacity improvement with base-station antenna arrays in cellular CDMA, *IEEE Trans. Veh. Tech.*, vol. 43, no. 3, pp. 691-698, Aug. 1994.
- [7] J. C. Liberti and T. S. Rappaport, Reverse channel performance improvements in CDMA cellular communication systems employing antenna arrays, *IEEE Trans. Veh. Tech.*, vol. 43, no. 3, pp. 680-690, Aug. 1994.
- [8] S. Talwar, M. Viberg, A. Paulraj, Blind separation of synchronous co-channel digital signals using an antenna array-Part I: Algorithms, *IEEE Trans. Signal Processing*, vol. 44, no. 5, pp. 1184-1197, May 1996.
- [9] A. L. Swindlehurst, S. Daas, and J. Yang, Analysis of a decision directed beamformer, *IEEE Trans. Signal Processing*, vol. 43, no. 12, pp. 2920-2927, Dec. 1995.
- [10] J. Litva and T. K-Y. Lo, *Digital Beamforming in Wireless Communications*, Artech House, 1996.
- [11] D. Gerlach and A. Paulraj, Adaptive transmitting antenna arrays with feedback, *IEEE Signal Processing Lett.*, vol. 1, no. 10, pp. 150-152, Oct. 1994.
- [12] G. Xu and H. Liu, An effective transmission beamforming scheme for frequency-division-duplex digital wireless communication systems, in *Proc. IEEE ICASSP-95*, pp. 1729-1732, 1995.
- [13] C. Farsakh and J. A. Nossek, Channel allocation and downlink beamforming in an SDMA mobile radio system, in *Proc. 6th IEEE PIMRC*, pp. 687-691, 1995.
- [14] P. Zetterberg and B. Ottersten, The spectrum efficiency of a base station antenna array system for spatially selective transmission, *IEEE Trans. Veh. Tech.*, vol. 44, no. 3, pp. 651-660, Aug. 1995.
- [15] R. Bernhardt, The use of multiple-beam directional antenna in wireless messaging systems, in *Proc. IEEE VTC-95*, pp. 858-861, Aug. 1995.
- [16] G. G. Raleigh, S. N. Diggavi, V. K. Jones, and A. Paulraj, A blind adaptive transmit antenna algorithm for wireless communication, in *Proc. IEEE ICC-95*, pp. 1494-1499, June 1995.
- [17] A. Klouche-Djedid and M. Fujita, Adaptive array sensor processing applications for mobile telephone communications, *IEEE*

저 자 소 개



吳 成 根(正會員)

1961년 4월 4일생. 1983년 2월 경북 대학교 전자공학과 졸업(공학사). 1985년 2월 한국과학기술원 전기 및 전자공학과 졸업(공학석사). 1990년 8월 한국과학기술원 전기 및 전자공학과 졸업(공학박사). 1993년 12월 - 1993년 8월 삼성전자(주). 1993년 9월 - 현재 아주대학교 전기전자공학부 조교수. 1996년 2월 - 1997년 1월 Simon Fraser 대학교(캐나다) 교환교수. 주관심분야는 이동통신 시스템용 Smart Antenna 시스템, 이동통신 시스템용 적응등화기, DS-CDMA 수신 시스템, Acoustic Echo Canceller

Shawn P. Stapleton

Ottawa / Carleton 대학교(공학사,공학석사,공학박사). 1982년 Engineer, Communication Research Center. 1983년 Microwave Engineer, Canadian Astronautics Ltd. 1984년 Consultant, Canadian Astronautics Ltd. 1986년 Senior Microwave Engineer, Communication Research Center. 1989년 Vice President, TRL, Canada. 1994년 - 현재 Professor, Engineering Science, Simon Fraser Univ.. 주관심분야는 Mobile Communication, Power Amplifier Linearization, Adaptive Array Antennas, RF/Microwave Circuit and Devices, Digital Signal Processing